FEBS Letters 586 (2012) 3692–3697

FEBS Letters

journal homepage: www.FEBSLetters.org

Glycine decarboxylase controls photosynthesis and plant growth

Stefan Timm [a], Alexandra Florian [b], Stephanie Arrivault [b], Mark Stitt [b], Alisdair R. Fernie [b], Hermann Bauwe [a,*]

[a] Plant Physiology Department, University of Rostock, D-18051 Rostock, Germany
[b] Max Planck Institute of Molecular Plant Physiology, D-14476 Golm, Germany

ARTICLE INFO

Article history:
Received 22 August 2012
Accepted 26 August 2012
Available online 11 September 2012

Edited by Ulf-Ingo Flügge

Keywords:
Photosynthesis
Photorespiration
Glycine decarboxylase
H-Protein
Arabidopsis

ABSTRACT

Photorespiration makes oxygenic photosynthesis possible by scavenging 2-phosphoglycolate. Hence, compromising photorespiration impairs photosynthesis. We examined whether facilitating photorespiratory carbon flow in turn accelerates photosynthesis and found that overexpression of the H-protein of glycine decarboxylase indeed considerably enhanced net-photosynthesis and growth of *Arabidopsis thaliana*. At the molecular level, lower glycine levels confirmed elevated GDC activity in vivo, and lower levels of the CO_2 acceptor ribulose 1,5-bisphosphate indicated higher drain from CO_2 fixation. Thus, the photorespiratory enzyme glycine decarboxylase appears as an important feed-back signaller that contributes to the control of the Calvin–Benson cycle and hence carbon flow through both photosynthesis and photorespiration.

1. Introduction

As a close partner of the Calvin–Benson (CB) cycle of photoautotrophic CO_2 fixation, the photorespiratory cycle is one of the major highways for the flow of carbon in the geo-biosphere. Briefly, this metabolic process starts when the key enzyme of the Calvin–Benson cycle, ribulose 1,5-bisphosphate (RuBP) carboxylase/oxygenase (Rubisco), covalently binds O_2 instead of CO_2 to RuBP [1]. Oxygenation of RuBP then produces one molecule each of 3-phosphoglycerate (3PGA) and 2-phosphoglycolate (2PG). In plants grown in normal air, the chance for binding CO_2 is only about twice as high as for O_2; that is, about every third to fourth molecule of RuBP becomes oxygenated [2]. Consequently, most land plants produce huge amounts of 2PG every day, which cannot directly re-enter the CB cycle and is also a potent inhibitor of enzymes of the CB cycle [3,4]. It is scavenged by the photorespiratory cycle, which combines two molecules of 2PG to one molecule of 3PGA, releasing one molecule of CO_2 [5–7]. Over decades, much effort has been spent to engineer Rubisco with less oxygenase activity [8], reduce photorespiratory CO_2 losses by increasing re-assimilation [9] or improve C_3 photosynthesis by other means [10,11]. The most ambitious contemporary project in this context is directed towards engineering a CO_2-concentrating C_4 rice variant [12].

Photorespiration is a universal and vital feature of all oxygenic autotrophs including cyanobacteria, green microalgae, and C_4 plants [13–15]. Intriguingly, even small impairments of photorespiratory carbon flow, may they be caused by chemical inhibitors [16] or genetic approaches [17,18], reduce photosynthetic CO_2 fixation. The mechanism of this feedback is not exactly known but could include inhibition of key enzymes of the CB cycle by photorespiratory metabolites such as 2PG [3,4], glyoxylate [19–21], and glycine [22]. We hypothesized that, if inhibition of the CB cycle by photorespiratory metabolites indeed represents a natural regulatory phenomenon, facilitating photorespiratory carbon flow should consequently improve photosynthetic CO_2 assimilation. To test this hypothesis, we selected the mitochondrial enzyme glycine decarboxylase (GDC) for an overexpression experiment. This particular enzyme was a prime candidate because it produces the photorespiratory CO_2 [23] and because the leaf glycine level is known as a sensitive indicator of altered photorespiratory carbon flow [24]. Mechanistically, GDC is a four-protein system comprising three enzymes (P-protein, T-protein, and L-protein) plus H-protein, a small lipoylated protein that commutes from one enzyme to the other. First, H-protein conveys the lipoyl-bound aminomethylene intermediate remaining after oxidative glycine decarboxylation from the P- to the T-protein. Eventually, in the reaction catalyzed by the L-protein, it donates reducing equivalents to NAD^+ and becomes re-oxidized.

Abbreviations: 3PGA, 3-phosphoglycerate; 2PG, 2-phosphoglycolate; CB, Calvin–Benson; GDC, glycine decarboxylase; RubP, ribulose 1,5-bisphosphate

* Corresponding author. Address: University of Rostock, Plant Physiology Department, Albert-Einstein-Straße 3, D-18051 Rostock, Germany. Fax: +49 (0)3814986112.
E-mail address: hermann.bauwe@uni-rostock.de (H. Bauwe).

0014-5793/$36.00
http://dx.doi.org/10.1016/j.febslet.2012.08.027

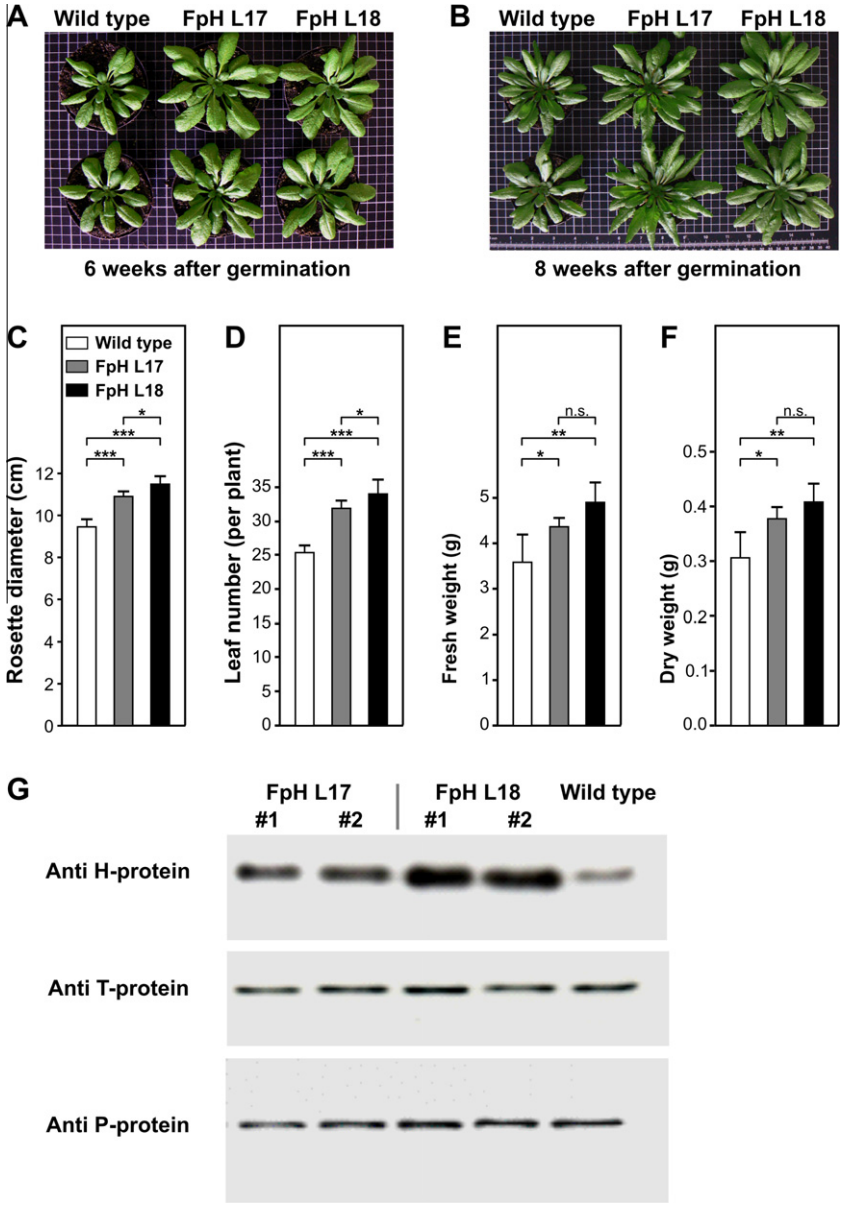

Fig. 1. H-protein overexpressors grow faster and produce more biomass. (A and B) Two individual plants each of the *Arabidopsis* wild type, FpH L17, and FpH L18 grown side-by-side for six and eight weeks. (C) Rosette diameters, (D) leaf numbers, (E) fresh weight, and (F) dry weight at growth stadium 5.1 [30]. Columns represent mean values ± SD (at least 5 individual plants for C, E and F; 25 individual plants for D). Asterisks indicate significant differences to the wild-type control or between lines FpH L17 and L18 ($^{*}p < 0.05$; $^{**}p < 0.01$; $^{***}p < 0.001$; n.s., not significant). (G) Immunoblots with antibodies against recombinant H-, T-, and P-protein, using 3 μg leaf protein per lane of a denaturing polyacrylamide gel and two plant individuals per overexpressor line. Data for two more lines, FpH L15 and L16, are shown in Supplementary Fig. 2.

2. Materials and methods

2.1. Overexpression constructs, transformation, and plant growth

The entire coding sequence for the GDC H-protein (*GLDH*) was PCR-amplified from *Flaveria pringlei* cDNA HFP4 [25] using primers FpGLDH-SacI-S (5′-GAG CTC ATG GCT CTT AGA ATC TGG GCT-3′) and FpGLDH-EcoRI-AS (5′-GAA TTC CTA CGTG AGC AGA ATC TTC TTC-3′). This amplificate was ligated into vector pGEMT (Invitrogen) and its correct sequence confirmed. The *Sac* I-*Eco* RI fragment was excised and ligated in front of the CaMV polyA site of the pGreen 35S-CaMV cassette (http://www.pgreen.ac.uk) to generate *GLDH:CaMV*. The *ST-LS1* promoter sequence [26] was PCR-amplified from vector L700-pBIN19 [17] using primers ST-LS1-SacI-S (5′-GAG CTC GGC TTG ATT TGT TAG AAA ATT-3′) and ST-LS1-BamHI-AS (5′-GGA TCC TTT CTC CTA TAC CTT TTT TCT-3′), ligated into the binary plant transformation vector pGreen0229 [27] via the introduced *Sac* I and *Bam* HI sites, and complemented with the GDC-H:CaMV fragment via *Bam* HI and *Eco* RV sites. This construct (schematically shown in Supplementary Fig. 1) was introduced into *Agrobacterium tumefaciens* strain GV3101 and used for the transformation [28] of *Arabidopsis thaliana* ecotype Col-0 (*Arabidopsis*). Twenty-two phosphinotricine (Basta) resistant lines were isolated and preselected according to their leaf GDC-H content. Then, stable T3 lines were generated, and four of these lines displaying intermediate (lines FpH L16 and L17) and high H-protein overexpression (lines FpH L15 and L18) selected for further examination. For all analyses, we used plants grown at environmentally controlled conditions (10/14 h day/night-cycle, 20/18 °C, ~150 μmol·m^{-2} s^{-1} photosynthetically active radiation) [29] to stadium 5.1 as defined in Boyes et al. [30].

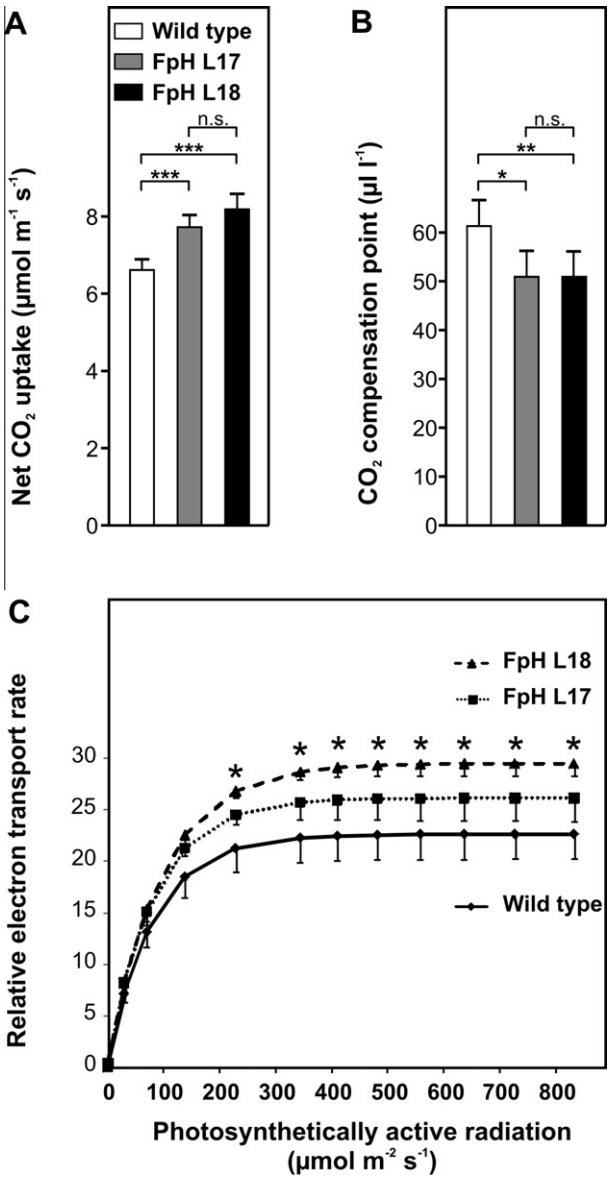

Fig. 2. H-protein overexpressors display higher CO_2 net-uptake rates, CO_2 compensation points and improved light response. (A) Photosynthetic net-CO_2 uptake rates at 400 µL L^{-1} CO_2 and 21% O_2. (B) CO_2 compensation points at 400 µL L^{-1} CO_2 and 21% O_2. (C) Relative electron transport rates at varying light intensity in air. Columns and data points represent mean values ± SD (at least 5 individual plants per line) for the wild type, FpH L17, and FpH L18. Asterisks indicate significant differences to the wild-type control or between FpH L17 and L18 ($^{*}p < 0.05$; $^{**}p < 0.01$; $^{***}p < 0.001$; n.s., not significant). Net CO_2 uptake rates and CO_2 compensation points for two more lines, FpH L15 and L16, are shown in Supplementary Fig. 2.

2.2. Immunological studies

SDS–PAGE of whole leaf protein extracts and protein gel blotting experiments were performed according to standard protocols using antibodies raised against recombinant H-protein (*Flaveria trinervia*), P-protein (*Flaveria anomala*), and T-protein (*Solanum tuberosum*).

2.3. Gas exchange and fluorescence measurements

Gas exchange measurements were performed as previously described [29]. Night-respiration rates were determined 4 h after switching off the lights during the normal day/night cycle. Maximum PSII quantum yields (F_v/F_m) and relative electron transport rates (ETR) at varying photosynthetic photon flux densities (PPFD) were measured using an Imaging PAM (M series, Walz, [31]). In short, basal fluorescence (F_0) was measured with dark-adapted leaves and steady-state fluorescence (F_s) with varying intensities of actinic light. Maximum fluorescence (dark-adapted leaves, F_m; illuminated leaves, F_m') was induced with saturating white-light pulses (5000 µmol m^{-2} s^{-1}). F_v/F_m was calculated as $(F_m - F_0)/F_m$ and the effective quantum yield of PSII as YPSII = $(F_m' - F_s)/F_m'$ according to Genty [32]. From these values, absolute electron transport rates were calculated as ETR = YPSII × PPFD × 0.84 × 0.5, assuming that 84% of the incident quanta are absorbed by the leaf and that linear electron transport requires two quanta per electron. The light saturation point (LSP) is the PPFD that causes 90% of the maximum ETR (ETR_{max}).

Table 1
PSII fluorescence parameters and relative photosynthetic electron transport. Data for maximum quantum efficiency of PSII (F_v/F_m), electron transport rate efficiency at low light intensity (alpha), maximum relative electron transport rate (ETR_{max}), and the light saturation point (LSP) are shown as mean values ± SD from at least five individual plants (5 areas of interest each per plant).

	Wild type	FpH L17	FpH L18
F_v/F_m	0.7572 ± 0.0172	0.7587 ± 0.0097	0.7662 ± 0.0041
Alpha	0.3107 ± 0.0406	0.3263 ± 0.0615	0.3089 ± 0.0431
ETR_{max}	23.12 ± 2.94	26.18 ± 2.48	29.49 ± 1.37*
LSP	171.68 ± 13.12	180.03 ± 28.58	202.97 ± 13.21*

Asterisks indicate significant differences relative to side-by-side grown wild-type plants ($^{*}p < 0.05$).

2.4. Metabolite profiling

Rosette leaf samples were harvested in the middle of the light period (after 5 h) and analyzed as described elsewhere for the GC–MS-based method [33] and for the LC–MS-based method [34].

2.5. Statistical analysis

Analysis of variance (ANOVA) was performed for all data using the Holm and Sidak test for comparisons (Sigma Plot 11, Systat Software Inc.).

3. Results and discussion

Since it is known that elevated H-protein concentrations increase P-protein activity in vitro [35], we chose this particular GDC component protein for overexpression in *Arabidopsis*. To avoid RNA interference and provide adequate transcriptional regulation, we fused cDNA encoding a *Flaveria pringlei* H-protein [25] to the leaf-specific and light-regulated *Solanum tuberosum ST-LS1* promoter [26] and used this construct to stably transform wild-type *Arabidopsis* [28]. Transgenic lines were preselected from a total of 22 Basta-resistant lines according to their leaf H-protein content and selfed over several generations. Two T3-generation lines displaying intermediate (line FpH L17) and high (line FpH L18) H-protein overexpression were examined for photosynthetic-photorespiratory properties, metabolite contents, and growth. A less comprehensive data set obtained with two more overexpressor lines (FpH L15 and L16) is shown in Supplementary Fig. 2. To exclude seed-age related bias, wild-type seed of the same harvest was used for growing the control plants.

In comparison to simultaneously (randomized side-by-side) grown wild-type *Arabidopsis*, a distinct growth promotion of the overexpressor lines became apparent already several weeks after germination and was fully established after six weeks (Fig. 1A

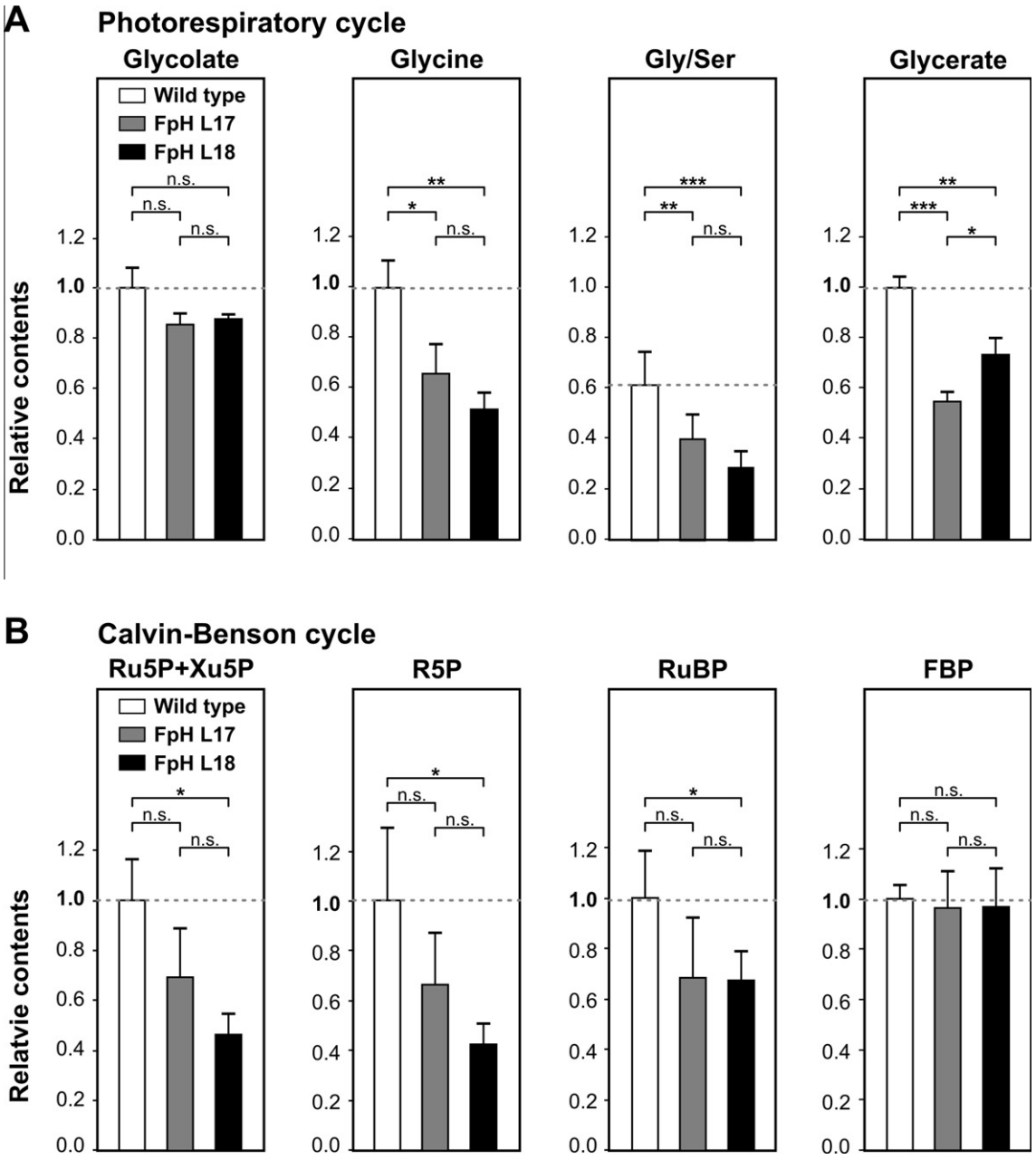

Fig. 3. H-protein overexpression accelerates the turnover of glycine and RuBP. Relative metabolite contents in leaf samples harvested at mid-day were determined by (A) GC–MS based metabolite profiling [33] and (B) LC–MS based metabolite profiling [34]. Full lists of metabolite changes are shown in Supplementary Tables 1 and 2. Columns represent mean values ± SD from at least 4 individual plants. Asterisks indicate significant differences to the wild-type control and between FpH L17 and L18 ($^{*}p < 0.05$; $^{**}p < 0.01$; $^{***}p < 0.001$; n.s., not significant).

and B). In quantitative terms, the overexpressor lines displayed significantly larger rosettes (Fig. 1C) and more leaves per plant (Fig. 1D) in combination with significantly longer (wild type, 3.75 ± 0.13; FpH L17, 3.98 ± 0.08; FpH L18, 4.34 ± 0.16 cm) and broader (wild type, 1.60 ± 0.15; FpH L17, 1.89 ± 0.10; FpH L18, 1.95 ± 0.07 cm) rosette leaves. These improved growth features summed up to 37% higher fresh (Fig. 1E) and 33% higher dry weight (Fig. 1F) in the best-performing line FpH L18. These growth features correlated nicely with about 2.5-fold (FpH L17) or fivefold (FpH L18) elevated leaf H-protein levels (Fig. 1G). Total leaf contents of P- and T-protein remained unaltered (Fig. 1G). Germination and the time until flowering were also unaltered relative to wild-type plants.

The improved growth of the H-protein overexpressor lines was associated with significantly accelerated net-CO_2 uptake rates (Fig. 2A and Supplementary Fig. 2). Moreover, we observed significantly lower CO_2 compensation points (Γ) in three out of four examined overexpressor lines (Fig. 2B and Supplementary Fig. 2). In land plants of the C_3 photosynthetic type, which include *Arabidopsis*, Γ is a very sensitive indicator of the balance between photosynthetic CO_2 uptake and (photo)respiratory CO_2 release. Our data suggest that this balance is affected by the catalytic capacity of the GDC reaction that, on its part, depends on the amount of available H-protein.

At a fivefold elevated CO_2 concentration, which considerably suppresses photorespiration, statistically significant differences in net-CO_2 uptake between the wild type and overexpressor lines could not be discerned any more (wild type, 13.39 ± 0.42; FpH L17, 13.83 ± 0.41; FpH L18, 13.94 ± 0.75). This further supports our notion that the enhanced photosynthetic

CO_2 uptake is the result of an alleviated photorespiratory carbon flow, brought about by higher GDC activity. Plant growth, to a large extent, occurs during the night and is driven by the use of accumulated stocks of transitional starch for respiration [36]. Hence, though we did not measure starch contents, the 20% (in FpH L17) and 24% (in FpH L18) enhanced rates of night respiration (wild type, 0.70 ± 0.07; FpH L17, 0.84 ± 0.17; FpH L18, 0.87 ± 0.09) fit nicely to the better plant growth demonstrated in Fig. 1A and B.

In order to examine whether these alterations in photosynthetic gas exchange affect the photosynthetic electron transport, we measured maximum PSII quantum yields (F_v/F_m) and relative electron transport rates (ETR) at varying light intensities (Fig. 2C). F_v/F_m values were very similar in the wild type and the overexpressor lines, but both the ETR values and the light saturation points were significantly higher in the plants containing more GDC H-protein, especially at high light intensities. This observation indicates that the improvements to the photosynthetic-photorespiratory carbon flow in turn cause an accelerated electron flow at PSII (Table 1).

An alleviation of a restriction in photorespiratory carbon flow should ultimately result in lower steady-state concentrations of photorespiratory metabolites. In the case of elevated GDC activity, one would anticipate reduced glycine levels. Indeed, metabolite profiling by GC–MS revealed an up to a significant 34–48% reduction of the leaf glycine content and the glycine-to-serine ratio in both overexpressor lines (Fig. 3A). Except some changes in the levels of several other photorespiratory metabolites upstream (non-significant 12–15% decrease of glycolate) and downstream (20–60% increase in hydroxypyruvate, significant 27–45% decrease of glycerate) of the GDC reaction, the levels of most other metabolites remained unaltered (Supplementary Table 1). The only other metabolites showing a significant change in both lines were asparagine and fructose.

Our hypothesis would also predict that the CO_2-fixing part of the CB cycle will become a stronger sink for RuBP once the hypothesized inhibition by photorespiratory metabolites is partially relieved. This is what we observed as well: changes to CB cycle metabolites were minor to nil – except considerably lower values for RuBP, pentulose 5-phosphates, and ribose 5-phosphate in the H-protein overexpressing lines (Fig. 3B and Supplementary Table 2). Again, this effect was approximately correlated with the amount of extra H-protein. The slight increase of fructose 6-phosphate, glucose 6-phosphate, and glucose 1-phosphate, which are intermediates in the pathway of sucrose synthesis, is consistent with the higher rates of photosynthesis.

Summarizing, our findings demonstrate regulatory interaction between the photorespiratory pathway and the CB cycle. A plausible explanation could be that some photorespiratory metabolites, for example glyoxylate or glycine, exert negative feed-back to down-regulate CB cycle enzymes. Our experiments suggest that this feed-back inhibition can be artificially relaxed by decreasing the accumulation of intermediates of the photorespiratory pathway, in particular at the glycine-to-serine conversion step. This effect is best visible by the reduced leaf content of glycine in combination with accelerated CO_2 fixation and a consequently lower RuBP level. From an ecophysiological point of view, the observed interaction might represent a useful strategy of C_3 plants to simultaneously down-regulate photosynthesis and photorespiration at high-photorespiration conditions, for example at high temperatures or suboptimum water supply. The operation and fine-tuning of this regulation remain to be investigated. We can currently only speculate on the actual regulator metabolite(s) and possible target enzyme(s) in the CB cycle; however, as far as the photorespiratory side is concerned, GDC appears as one of the key signallers in this network.

Acknowledgments

We thank Kathrin Jahnke for technical assistance and Martin Hagemann for helpful discussions and critically reading the manuscript. This work was supported by Grants from the Deutsche Forschungsgemeinschaft (Promics Photorespiration Network, FOR 1186) to A.R.F. and H.B.

Appendix A. Supplementary data

Supplementary data associated with this article can be found, in the online version, at http://dx.doi.org/10.1016/j.febslet.2012.08.027.

References

[1] Cleland, W.W., Andrews, T.J., Gutteridge, S., Hartman, F.C. and Lorimer, G.H. (1998) Mechanism of Rubisco: the carbamate as general base. Chem. Rev. 98, 549–562.
[2] Galmés, J., Flexas, J., Cifre, J., Medrano, H., Keys, A.J., Mitchell, R.A.C., Madgwick, P.J., Haslam, R.P. and Parry, M.A.J. (2005) Rubisco specificity factor tends to be larger in plant species from drier habitats and in species with persistent leaves. Plant Cell Environ. 28, 571–579.
[3] Anderson, L.E. (1971) Chloroplast and cytoplasmic enzymes. 2. Pea leaf triose phosphate isomerases. Biochim. Biophys. Acta 235, 237–244.
[4] Kelly, G.J. and Latzko, E. (1976) Inhibition of spinach-leaf phosphofructokinase by 2-phosphoglycollate. FEBS Lett. 68, 55–58.
[5] Foyer, C.H., Bloom, A.J., Queval, G. and Noctor, G. (2009) Photorespiratory metabolism: genes, mutants, energetics, and redox signaling. Annu. Rev. Plant Biol. 60, 455–484.
[6] Tolbert, N.E. (1997) The C_2 oxidative photosynthetic carbon cycle. Annu. Rev. Plant Physiol. Plant Mol. Biol. 48, 1–25.
[7] Bauwe, H., Hagemann, M. and Fernie, A.R. (2010) Photorespiration: players, partners and origin. Trends Plant Sci. 15, 330–336.
[8] Whitney, S.M., Houtz, R.L. and Alonso, H. (2011) Advancing our understanding and capacity to engineer nature's CO_2-sequestering enzyme. Rubisco. Plant Physiol. 155, 27–35.
[9] Maurino, V.G. and Peterhänsel, C. (2010) Photorespiration: current status and approaches for metabolic engineering. Curr. Opin. Plant Biol. 13, 248–255.
[10] von Caemmerer, S. and Evans, J.R. (2010) Enhancing C_3 photosynthesis. Plant Physiol. 154, 589–592.
[11] Raines, C.A. (2011) Increasing photosynthetic carbon assimilation in C_3 plants to improve crop yield: current and future strategies. Plant Physiol. 155, 36–42.
[12] Hibberd, J.M., Sheehy, J.E. and Langdale, J.A. (2008) Using C_4 photosynthesis to increase the yield of rice – rationale and feasibility. Curr. Opin. Plant Biol. 11, 228–231.
[13] Eisenhut, M., Ruth, W., Haimovich, M., Bauwe, H., Kaplan, A. and Hagemann, M. (2008) The photorespiratory glycolate metabolism is essential for cyanobacteria and might have been conveyed endosymbiontically to plants. Proc. Natl. Acad. Sci. USA 105, 17199–17204.
[14] Hackenberg, C., Kern, R., Hüge, J., Stal, L.J., Tsuji, Y., Kopka, J., Shiraiwa, Y., Bauwe, H. and Hagemann, M. (2011) Cyanobacterial lactate oxidases serve as essential partners in N_2 fixation and evolved into photorespiratory glycolate oxidases in plants. Plant Cell 23, 2978–2990.
[15] Zelitch, I., Schultes, N.P., Peterson, R.B., Brown, P. and Brutnell, T.P. (2009) High glycolate oxidase activity is required for survival of maize in normal air. Plant Physiol. 149, 195–204.
[16] Servaites, J.C. and Ogren, W.L. (1977) Chemical inhibition of the glycolate pathway in soybean leaf cells. Plant Physiol. 60, 461–466.
[17] Heineke, D., Bykova, N., Gardeström, P. and Bauwe, H. (2001) Metabolic response of potato plants to an antisense reduction of the P-protein of glycine decarboxylase. Planta 212, 880–887.
[18] Wingler, A., Lea, P.J. and Leegood, R.C. (1997) Control of photosynthesis in barley plants with reduced activities of glycine decarboxylase. Planta 202, 171–178.
[19] Chastain, C.J. and Ogren, W.L. (1989) Glyoxylate inhibition of ribulosebisphosphate carboxylase/oxygenase activation state in vivo. Plant Cell Physiol. 30, 937–944.
[20] Campbell, W.J. and Ogren, W.L. (1990) Glyoxylate inhibition of ribulosebisphosphate carboxylase/oxygenase activation in intact, lysed, and reconstituted chloroplasts. Photosynth. Res. 23, 257–268.
[21] Häusler, R.E., Bailey, K.J., Lea, P.J. and Leegood, R.C. (1996) Control of photosynthesis in barley mutants with reduced activities of glutamine synthetase and glutamate synthase. 3. Aspects of glyoxylate metabolism and effects of glyoxylate on the activation state of ribulose-1,5-bisphosphate carboxylase–oxygenase. Planta 200, 388–396.
[22] Eisenhut, M., Bauwe, H. and Hagemann, M. (2007) Glycine accumulation is toxic for the cyanobacterium *Synechocystis* sp. strain PCC 6803, but can be compensated by supplementation with magnesium ions. FEMS Microbiol. Lett. 277, 232–237.

[23] Kisaki, T. and Tolbert, N.E. (1970) Glycine as substrate for photorespiration. Plant Cell Physiol. 11, 247–258.
[24] Blackwell, R.D., Murray, A.J.S., Lea, P.J., Kendall, A., Hall, N.P., Turner, J.C. and Wallsgrove, R.M. (1988) The value of mutants unable to carry out photorespiration. Photosynth. Res. 16, 155–176.
[25] Kopriva, S. and Bauwe, H. (1995) H-protein of glycine decarboxylase is encoded by multigene families in *Flaveria pringlei* and *F. cronquistii* (Asteraceae). Mol. Gen. Genet. 248, 111–116.
[26] Stockhaus, J., Schell, J. and Willmitzer, L. (1989) Correlation of the expression of the nuclear photosynthetic gene *ST-LS1* with the presence of chloroplast. EMBO J. 8, 2445–2451.
[27] Hellens, R.P., Edwards, E.A., Leyland, N.R., Bean, S. and Mullineaux, P.M. (2000) PGreen: a versatile and flexible binary Ti vector for *Agrobacterium*-mediated plant transformation. Plant Mol. Biol. 42, 819–832.
[28] Clough, S.J. and Bent, A.F. (1998) Floral dip: a simplified method for *Agrobacterium*-mediated transformation of *Arabidopsis thaliana*. Plant J. 16, 735–743.
[29] Timm, S., Florian, A., Jahnke, K., Nunes-Nesi, A., Fernie, A.R. and Bauwe, H. (2011) The hydroxypyruvate-reducing system in *Arabidopsis*: Multiple enzymes for the same end. Plant Physiol. 155, 694–705.
[30] Boyes, D.C., Zayed, A.M., Ascenzi, R., McCaskill, A.J., Hoffman, N.E., Davis, K.R. and Gorlach, J. (2001) Growth stage-based phenotypic analysis of Arabidopsis: A model for high throughput functional genomics in plants. Plant Cell 13, 1499–1510.
[31] Schreiber, U., Schliwa, U. and Bilger, W. (1986) Continuous recording of photochemical and nonphotochemical chlorophyll fluorescence quenching with a new type of modulation fluorometer. Photosynth. Res. 10, 51–62.
[32] Genty, B., Briantais, J.M. and Baker, N.R. (1989) The relationship between the quantum yield of photosynthetic electron transport and quenching of chlorophyll fluorescence. Biochim. Biophys. Acta 990, 87–92.
[33] Lisec, J., Schauer, N., Kopka, J., Willmitzer, L. and Fernie, A.R. (2006) Gas chromatography mass spectrometry-based metabolite profiling in plants. Nat. Protoc. 1, 387–396.
[34] Arrivault, S., Guenther, M., Ivakov, A., Feil, R., Vosloh, D., van Dongen, J.T., Sulpice, R. and Stitt, M. (2009) Use of reverse-phase liquid chromatography, linked to tandem mass spectrometry, to profile the Calvin cycle and other metabolic intermediates in Arabidopsis rosettes at different carbon dioxide concentrations. Plant J. 59, 826–839.
[35] Hasse, D., Mikkat, S., Hagemann, M. and Bauwe, H. (2009) Alternative splicing produces an H-protein with better substrate properties for the P-protein of glycine decarboxylase. FEBS J. 276, 6985–6991.
[36] Weise, S.E., Weber, A.P. and Sharkey, T.D. (2004) Maltose is the major form of carbon exported from the chloroplast at night. Planta 218, 474–482.